



**HAL**  
open science

## Thermal regime variability of islands in the Lena River near Yakutsk, eastern Siberia

François Costard, Emmanuèle Gautier, Pavel Konstantinov, Frederic Bouchard, Antoine Séjourné, Laure Dupeyrat, Alexander Fedorov

► **To cite this version:**

François Costard, Emmanuèle Gautier, Pavel Konstantinov, Frederic Bouchard, Antoine Séjourné, et al.. Thermal regime variability of islands in the Lena River near Yakutsk, eastern Siberia. *Permafrost and Periglacial Processes*, 2022, 33 (1), pp.18-31. 10.1002/ppp.2136 . hal-03821050v2

**HAL Id: hal-03821050**

**<https://hal.science/hal-03821050v2>**

Submitted on 26 Sep 2023

**HAL** is a multi-disciplinary open access archive for the deposit and dissemination of scientific research documents, whether they are published or not. The documents may come from teaching and research institutions in France or abroad, or from public or private research centers.

L'archive ouverte pluridisciplinaire **HAL**, est destinée au dépôt et à la diffusion de documents scientifiques de niveau recherche, publiés ou non, émanant des établissements d'enseignement et de recherche français ou étrangers, des laboratoires publics ou privés.

1 **Thermal regime variability of islands in the Lena River near Yakutsk, eastern Siberia**

2

3 **F. Costard<sup>1</sup>, E. Gautier<sup>2</sup>, P. Konstantinov<sup>3</sup>, F. Bouchard<sup>1</sup>, A. Séjourné<sup>1</sup>, L. Dupeyrat<sup>1</sup>, and A. Fedorov<sup>3</sup>**

4 <sup>1</sup> *Université Paris-Saclay, CNRS, GEOPS, UMR 8148, rue du Belvédère, 91405 Orsay, France.*

5 <sup>2</sup> *Université Paris 1 Panthéon-Sorbonne et CNRS UMR 8591, Laboratoire de Géographie*  
6 *Physique, Meudon, France*

7 <sup>3</sup> *Melnikov Permafrost Institute, RAS Siberian Branch, Yakutsk, Russia*

8

9 **Abstract**

10 Recent evidence has shown that Arctic regions have warmed about twice as much as elsewhere on the  
11 planet over the last decades, and that high-latitude permafrost-periglacial processes and hydrological  
12 systems are notably responsive to rising temperatures. The aim of this paper is to report on thermal  
13 regime of islands located along the Lena River floodplain, upstream of the city of Yakutsk (eastern  
14 Siberia). Four islands were monitored using waterproof dataloggers and continuous monitoring of  
15 frozen soil in contact with ice breakup of the Lena River. For each of these islands, we measured: i)  
16 ground surface temperature, air and frozen soil temperatures at different depths; ii) submersion  
17 duration during the flood. Our results show that within a zone of thick and continuous permafrost, the  
18 Lena floodplain is notably heterogeneous, with a combination of permanently and seasonally frozen  
19 islands. The ice breakups seem to have a negligible impact on the ground thermal regime. Our study  
20 confirms that relatively young (less than 30 years old) islands, composed of fine sand material, appear  
21 less prone to permafrost formation compared to older islands with ice-rich silty material.

22

23 **1. Introduction**

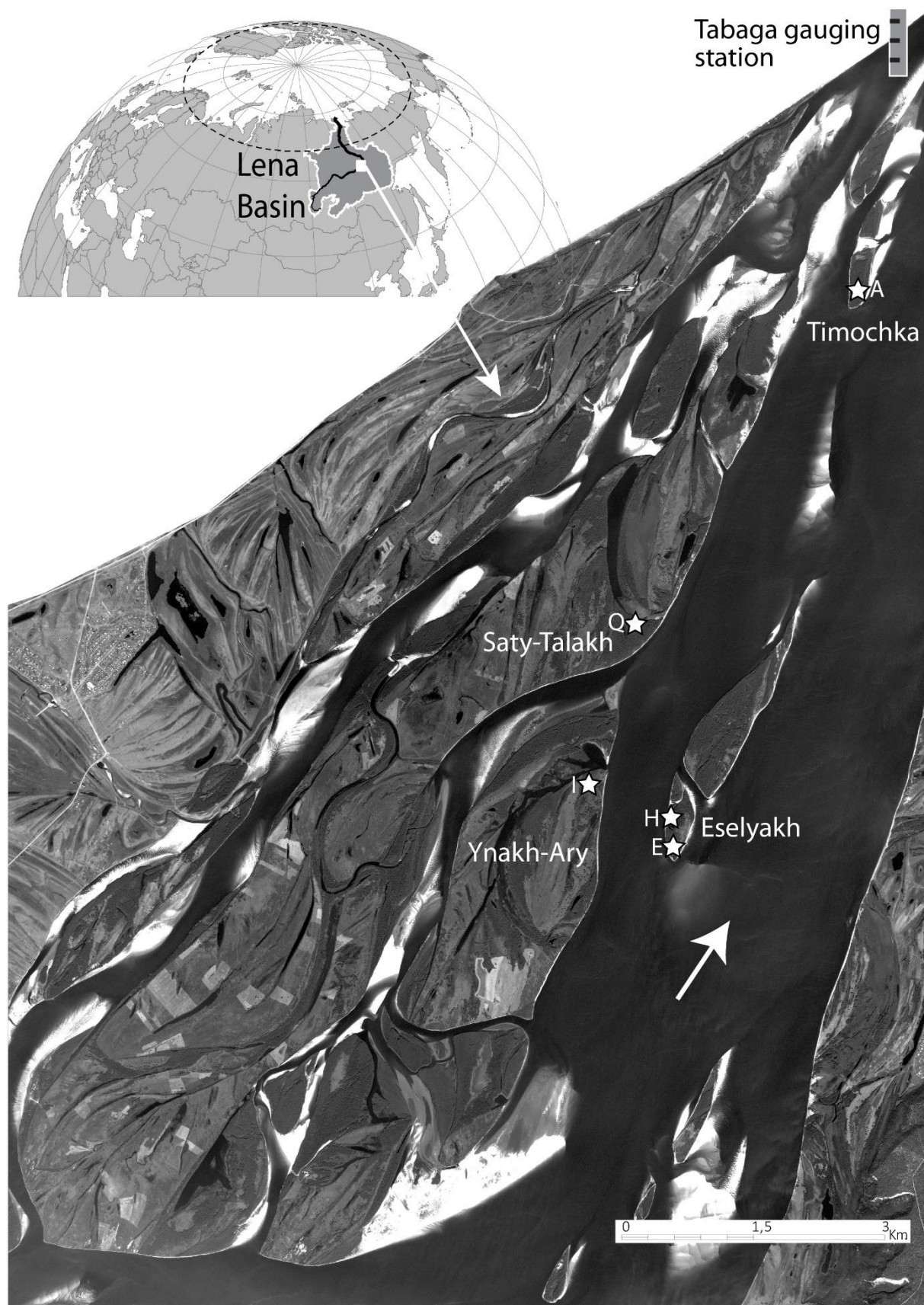
24

25 Permafrost has been warming at the global scale over the last decade, following the Arctic  
26 amplification of air temperature increase in the Northern Hemisphere (Biskaborn et al., 2019). Recent  
27 work has shown a significant increase in air and ground temperatures in central Yakutia (Eastern  
28 Siberia) since the late 1980s (Fedorov et al., 2014; Iijima et al., 2016, Zhang et al., 2012). In the Lena  
29 River valley (Figure 1), according to Iijima et al. (2010), the mean annual ground temperature at a depth  
30 of 3.2 m has increased by about 1.3°C since 1930. The mean annual air temperature at Yakutsk was -  
31 9.9°C and it ranged between -8°C and -12°C for the period 1936-199. The mean annual air temperature  
32 has increased to -8.4°C between 2000 and 2007 and to -7.4°C after 2008 (the last period ranging  
33 between -6.7°C and -7.8°C). A wetter period is registered between 2002 and 2008 (mean annual value  
34 for the period: 276 mm), however the precipitation has decreased after (about 220 – 230 mm). Very

35 wet conditions occurred in 1999, 2003, 2005, 2006, 2007 and 2013, with storms affecting Siberia  
36 resulting in more abundant late summer precipitation and early winter snow (Fedorov et al., 2014b;  
37 Iijima et al., 2016).  
38 Furthermore, active layer deepening results in an increase in river discharge (Peterson et al., 2002).  
39 More recently, Gautier et al. (2018) reported a strong water discharge increase since the beginning of  
40 the 21<sup>st</sup> century for the Lena River at Tabaga (just upstream of Yakutsk city, at 61° 4'N and 129° 3'E,  
41 Figure 1): the 2000-2017 discharge was 15% higher than the discharge for 1936-1999. Furthermore,  
42 floods are also changing, with more frequent flood peaks and longer recorded flooding durations  
43 (Gautier et al., 2018). Recent exceptional flood events are reported (Shiklomanov and Lammers, 2009;  
44 Costard et al., 2014; Gautier et al., 2018; Tei et al., 2020). There has also been a decrease in winter  
45 river ice cover, used as road. Winter thawing/melting events, as well as spring ice jam floods during  
46 the ice breakups represent major risks for riverside residents, road and river infrastructures. All these  
47 factors lead to permafrost instability and consequent changes in forest, wetland, lake and river  
48 ecosystems.

49

50



51  
 52 Figure 1: A: Location of the Lena basin and the study sites (upstream of Yakutsk). B: Observation points.  
 53 Star with letters: Data loggers; Background image: Spot 2008 (CNES, France).

54 Very few studies have focused on permafrost in floodplains and little is known on geomorphological  
55 impacts of ice breakups and floods on major Arctic rivers. Most of the geomorphological studies report  
56 on river dynamics of breakup for Canadian Arctic rivers (Beltaos and Burrell, 2002). Specifically, studies  
57 have shown the role of the ice cover and its thickness on the intensity of ice jams produced by ice packs  
58 along the Yukon River (Shen, 2003; Walker and Hudson, 2003). With increasing discharge, the ice cover  
59 under pressure locally cracks and starts to move (Shen, 2003). This is the beginning of the "breakup"  
60 phase where ice rafts accumulate at the head of islands (Figure 2); ice breakup usually occurs in spring,  
61 between May 20<sup>th</sup> and early June on the middle Lena River, and in Mid-June or late June downstream,  
62 in the low valley (Gautier and Costard, 2000). The flow often carries these ice blocks along with tree  
63 trunks (Walker and Hudson, 2003). Ice jams produce local dams, resulting in a sudden rise of water  
64 levels (Billfalk, 1982; Beltaos and Burell, 2002; Costard et al., 2014). During the flood season from May  
65 to July, the stream water warms the frozen soils, leading to accelerated erosion of the banks (Are,  
66 1983; Jahn, 1975; Walker, 1983). Melting of the ice contained in the porous sediment of the riverbank  
67 reduces its strength, and produces removable unconsolidated material (Costard et al., 2003).  
68 Furthermore, when the water level is above the bankfull level, the overbank water submerges the  
69 island soil that is still frozen. The effects of the submersion have never been studied.

70  
71 Breakups and floods are strongly heterogeneous, as numerous factors control their starting date,  
72 duration and intensity (Costard et al., 2014; Gautier et al., 2018). The flood wave coming from the  
73 upper basin can occur on a floodplain that is still frozen or not (depending on the local temperature).  
74 Moreover, analysis of climatic and hydrological data near Yakutsk showed a very clear thinning trend  
75 in winter ice thickness and a significant increase in water temperature of the Lena River near Tabaga  
76 (gauging station upstream section of Yakutsk, Figure 1). We have also demonstrated the impact of  
77 recent warming on increasing erosion rates of the islands by thermal erosion (Costard et al., 2007;  
78 Gautier et al., 2021).

79 Only a few studies report on permafrost thermal regime in Arctic floodplains, and in spite of a relatively  
80 good understanding of the initial stage of the breakup period of these periglacial rivers [Beltaos and  
81 Burrell, 2002; Shen, 2003; Billfalk, 1982], little is known regarding the influence of ice breakup and  
82 flooding on ground thermal regime during the flood season (Are, 1983; Walker, 1983). The major  
83 influence of water stream temperature on the thermal regime of frozen ground has already been  
84 demonstrated using cold room experiments (Costard et al., 2003), but only for river bank erosion.

85 Moreover, breakup and large flooding events represent an important risk in Arctic regions and can  
86 threaten infrastructures. In May 2001 and 2010, catastrophic breakup events linked to an early spring  
87 season following a severe winter strongly impacted the cities of Yakutsk and Lensk (Gautier et al.,  
88 2018). Recently, a project of a 6 km-long bridge across the Lena floodplain at Tabaga site is projected



89 and it implies accurate knowledge of the formation, and especially of the causes of the variable  
90 intensity of these ice breakups.

91



92

93 Figure 2: Beginning of the ice breakup on the Lena River, May 15<sup>th</sup>, 2010. Flow from right to left. During  
94 the first days, drifting ice blocks on the river formed thick ice accumulations at the head of Timochka  
95 Island, which led to a frontal erosion of up to 40 m within a few days.

96

97 The main objective of this paper is to analyze the near-surface thermal regime of four islands in the  
98 Lena River floodplain, eastern Siberia, and to determine to what extent it is affected by island dynamics  
99 and ice breakup/flooding events. We investigate the thermal influence of the water stream  
100 temperature by a vertical variation of the ground thermal regime during a typical submersion of the  
101 islands affected by ice breakups and flooding events.

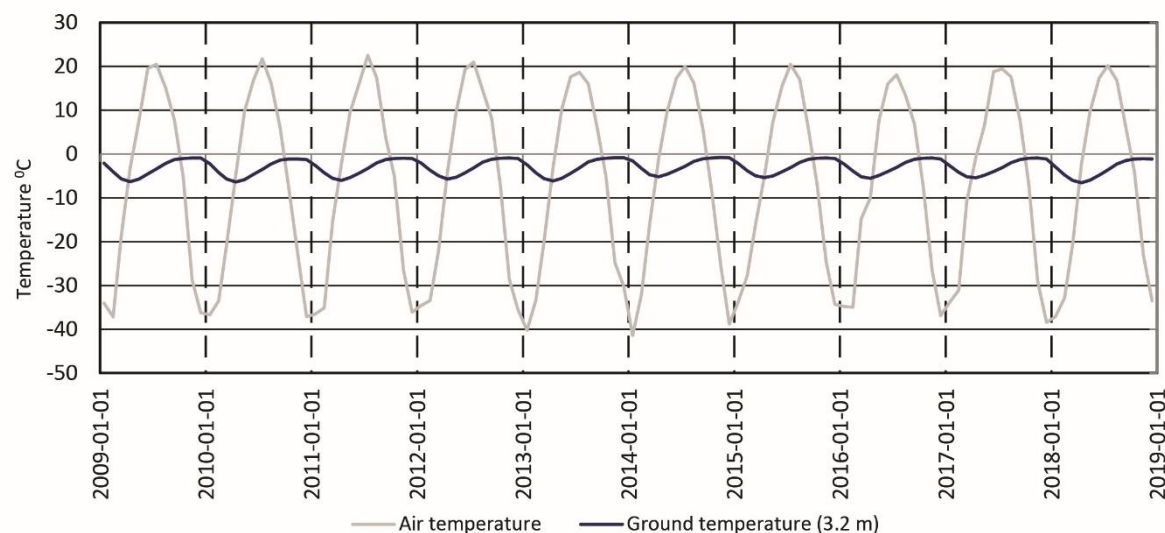
102

## 103 2. Study area

104 Central Yakutia (eastern Siberia) is characterized by a continental periglacial climate with extreme  
105 variations in air temperatures, ranging from +30°C in summer to -50°C in winter (Fedorov et al., 2014)  
106 (see Figure 3 for the period 2009-2018). The region is characterized by a thick continuous ice-rich  
107 permafrost of late Pleistocene age, called “Yedoma” (Antonov, 1960; Schirrmeyer et al., 2013). The  
108 mean air temperature at Yakutsk is -8.5 °C since the beginning of the 21<sup>st</sup> century. The winter  
109 temperature (October to April) ranged between -10°C and -40°C (Figure 3). The temperature becomes  
110 positive at the beginning of May and the mean monthly temperature can exceed +20°C from mid-June  
111 to mid-August. The low annual precipitation (230 mm near Yakutsk), together with a high evaporation  
112 rate, induces a dry climate (Antonov, 1960). Most of the precipitation occurs in summer, with 140 mm  
113 distributed between June and September. Snow cover thickness remains low (30 to 40 cm), which  
114 favors efficient frost penetration and the existence of a deep permafrost, especially underneath the  
115 taiga. The mean annual temperature of the permafrost at depths of 10 m to 20 m ranges from -2°C to

116 -4°C (Fedorov and Konstantinov, 2003). Since the end of the 1980s, it has undergone a warming of  
117 almost 1.5°C (at a depth of 3.2 m), together with a deepening of the active layer, with values ranging  
118 from 0.8 to 1.2 m at the latitude of Yakutsk (Fedorov and Konstantinov, 2003; Fedorov et al., 2014).

119  
120



121  
122

123 Figure 3: Mean monthly air and ground (3.2-m depth) temperature at Yakutsk (NOAA data) – July 2009  
124 – July 2018.

125  
126

127 The Lena River is one of the largest fluvial hydrosystems within the periglacial zone (Figure 1), with  
128 thick and continuous permafrost that covers 77% of the basin (Soloviev, 1973). During the winter  
129 season (October to April), the river flows under an ice cover with an average thickness of 1.4 m (min:  
130 0.3 m; max. 2 m). The river discharge is then extremely low (less than  $1500 \text{ m}^3 \text{ s}^{-1}$  at the Tabaga station,) and reaches its lowest discharge of  $870 \text{ m}^3 \text{ s}^{-1}$  in April, at the end of the winter (Gautier and Costard, 2000; Gautier et al., 2018). The breakup and the flood occur between May 20<sup>th</sup> and June 10<sup>th</sup>. However, the recent years showed earlier or later events (Gautier et al., 2018). The overbank discharge (about  $30\,000 \text{ m}^3 \cdot \text{s}^{-1}$  at Tabaga) inundates the forested islands and the floodplain with a great irregularity: the inundation can last from a few days to one month. After the flood, the water level rapidly drops in July. On the Lena River, ice breakups are controlled by the meridian course of the river, with a 30- to 50-day lag between basin upstream and downstream (Gautier et al., 2003). As a result, when snow and ice covers melt, a flood wave propagates from the southern regions further to the still-frozen regions in the north. Therefore, the water discharge increases abruptly and massive ice and log jams can be formed on the island heads (figure 2). Within a few days, the volume of water flow increases 20 to 45 times (Gautier et al., 2018). The peak flood can reach up to  $50,000 \text{ m}^3 \text{ s}^{-1}$  (Antonov, 1960, Liu et al., 2005; Gautier et al., 2018). At the latitude of Yakutsk, the water level during the flood season can be

143 up to 8 to 10 m higher than during the winter low water level (Costard et al., 2007; Gautier et al., 2018).  
144 During high floods, the Lena flood spreads over a width of 15 km. The water stream temperature,  
145 about 0°C in the winter and up to 8°C at the beginning of the flooding season, increases rapidly to  
146 reach 17-18°C in July and August (Costard et al., 2014).

147  
148 For the purpose of our study, a site upstream of Yakutsk (Figure 1) have been chosen, in order to avoid  
149 the urban heat flow. In addition, the upstream Lena River is not impacted by dams. Ten islands were  
150 preselected in the riverbed upstream of Tabaga gauging station, and four of them were instrumented  
151 and are discussed further in this paper (Figure 1). Eselyakh and Timochka islands (0.2 and 0.7 km<sup>2</sup> are  
152 located in the central part of the active channel, whereas Ynakh-Ary and Saty-Talakh are two much  
153 larger lateral islands, sizing 5 km<sup>2</sup> and 20 km<sup>2</sup>, respectively (Table 1). The island elevation ranges  
154 between 92 masl for the highest parts (levees and center of old islands) and 88 masl for the depressions  
155 that generally correspond to abandoned channels. The islands are colonized by a homogeneous alluvial  
156 forest mainly composed of willows. On the Lena River, islands are formed by stabilization of sand bars  
157 by pioneer sequences. Because of their abundance, young trees trap the sediment load, causing rapid  
158 vertical accretion of the island (Gautier et al., 2021). Hence, the base of the island stratigraphy is mainly  
159 composed of homometric ( $D_{50} = 200 - 250 \mu\text{m}$ ) sandy material organized in horizontal beds several  
160 tens of centimeters thick. The sandy deposits are often covered with layers of fine sand and silt ( $D_{50} =$   
161  $50 - 100 \mu\text{m}$ ) deposited by overbank flows. On the oldest islands, overbank deposits can be 2 m thick.  
162 Fine-grained deposits mixed with organic matter are found in abandoned channels. For a detailed  
163 description of the sedimentary sequences of these islands, see Gautier and Costard (2000), Costard et  
164 al. (2014), and Gautier et al. (2021).

165  
166 Bank erosion of the Lena river ranges on average between 11 and 18 m yr<sup>-1</sup> on island head (upper part)  
167 and 5 to 10 m on island side. In localized areas, erosion rates of 25 to 40 m yr<sup>-1</sup> could be observed  
168 (Gautier et al., 2003; Costard et al., 2007, 2014; Tananaev, 2016; Dupeyrat et al., 2018; Gautier et al.,  
169 2021). The thermo-mechanical process explains the relative efficiency of bank retreat (Walker and  
170 Arnborg, 1963; Jahn, 1975; Walker, 1983; Costard et al., 2014).

171

172

### 173 **3. Methods**

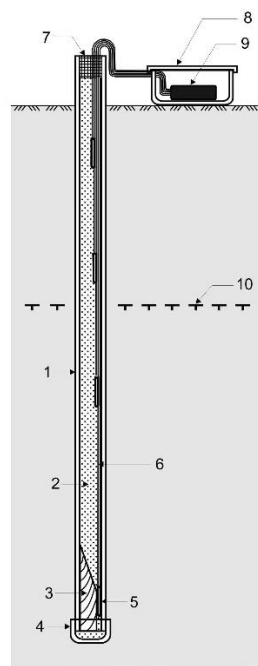
174 In order to determine the ground temperature and to evaluate the active layer thickness on the islands,  
175 various methods were integrated. First, a drilling campaign (2008) enabled the installation of several  
176 temperature sensors at different depths and a precise measurement of the active layer with a steel  
177 stick. Thus, topographic conditions do not change a lot in the proximity of the sensors. We used HOBO



178 4-channels dataloggers (model U12-008) to record variations in the thermal profile. Each datalogger,  
179 previously calibrated in the laboratory, includes 4 thermistor sensors (TMCx-HD) that produce a  
180 temperature-dependent voltage, which is then converted to temperature and stored in the datalogger,  
181 every hour, with an accuracy of  $\pm 0.25^{\circ}\text{C}$ , in the soil, at 0 m (soil surface), 1 m, 2 m and 3.2 m depth  
182 (Figure 4). On Saty-Talakh island, the sensors have been installed at 2 m, 3 m and 4 m depth (plus the  
183 surface). The annual periods are delimited from July to July. Once a year, after the ice breakup, we  
184 went to the instrumented sites to collect data from the dataloggers and to ensure the equipment  
185 maintenance on site. During the first year (2008) on Timochka and Eselyakh islands, only two among  
186 the four sensors worked well and the others were broken by the strong ice breakup. They were  
187 modified to ensure waterproof conditions and to improve the robustness of the equipment in order  
188 to control the mechanical effect of ice breakups (e.g., internal pressure). Thus, we had to develop a  
189 new system (Figure 4) that is much more efficient and could resist the repeated impacts of ice rafts  
190 and water pressure (Konstantinov et al., 2011). Unfortunately, because of the extremely rough  
191 conditions, the duration of measurements of the temperature sensors is very variable (Table 1): some  
192 of them have been working for more than 10 years, whereas others disappeared during a flood or were  
193 buried under meters of sediment and woody debris. Due to some severe breakups, some ground  
194 temperature sensors were broken during the first year. In the present study, we present the data of  
195 the devices that were installed several dozen meters away from the riverbank and that were preserved  
196 from erosion and/or thick sediment deposition during floods.

197

198



199

200 Figure 4: Sketch on the left: Drilling in the frozen soil for the installation of thermistor sensors placed  
 201 at 0 m (soil surface), 1 m, 2 m and 3.2 m depth. 1- polypropylene tube; 2- dry sand; 3-wooden bloc; 4-  
 202 tube plug; 5-sensor; 6-cable; 7- waterproofing compound; 8-protective box; 9-data logger; 10-bottom  
 203 of active layer. Photo on the right: HOBO datalogger modified to resist flooding of the island during  
 204 spring breakup. Note the two weights on the box and the wooden support holding the datalogger in  
 205 the waterproof box. (Figure modified from Konstantinov et al., 2011). Every sensor position was  
 206 precisely determined with a GPS and a total station.

207  
 208 The water levels and the daily discharge were recorded at Tabaga (gauging station, 8 km north from  
 209 the sites, see Figure 1). The overbank discharge and the submersion duration of the islands have been  
 210 determined during field observations during the flooding season. Island inundation begins when the  
 211 river discharge reaches about  $30\,000\text{ m}^3\cdot\text{s}^{-1}$  (Costard et al., 2014 and Gautier et al., 2001; Tananaev,  
 212 2016). The lowest parts of the islands can be inundated for a discharge a bit lower and the highest  
 213 parts need about  $32\,000\text{ m}^3\cdot\text{s}^{-1}$  to be flooded.

214

215 Table 1: Main features of the four study islands. Letters: temperature sensors.

Island Name	Area (m <sup>2</sup> )			Age	Dataloggers			Geomorphic Unit
	1967	2008	2017		Mean temp. at -3.2 m (°C)	Duration of measurement	Sediment	
<b>Eselyakh</b> – Upstream part Downstream part	486,726 416,877	198,256 790,189	105,520 675,931	> 60 yr	E: -2.2 H: -0.4	2008 – 2011 2008 – 2011	Mixed sed. Sand	Abandoned channel Bar/island
<b>Timochka</b> - Upstream part Downstream part	216,239 0	135,560 70,300	107,161 79,164	< 30 yr	A: 1.2	2008 – 2014	Sand	Bar/island
<b>Ynakh-Ary</b>	5047,718	5338,126	50294,298	> 70 yr	I: -3.9	2009 – 2016	Mixed sed.	Abandoned channel
<b>Saty-Talakh</b>	18 247,279	20 125,713	19 685,946	> 70 yr	Q: -0.6	2009 – 2018	Sand	Bar/island

216

217 We estimated the age of the islands based on the year of their appearance from a previous pluri-  
 218 decadal analysis of aerial pictures and satellite images (Figure 1 and Table 2) used by Gautier et al.  
 219 (2021). We also used the dendrochronology method to precisely measure the age of the oldest trees.  
 220 Our objectives were to determine whether the thermal regime is related to the age (and/or size) of  
 221 the islands.

222 For each of these sites, we also did an analysis of the sediments and stratigraphy using a soil moisture  
 223 sensor and grain-size was determined with a laser granulometer (see Supplementary material S1). The

224 depth of the permafrost table and its ice content were obtained by sampling with a drilling machine  
225 down to 3.2 m; the permafrost table was also measured every year with a stick. The analysis of the  
226 sediments was done at the Melnikov Permafrost Institute in Yakutsk.

227

## 228 4. Results

229 The analysis reveals an important inter-annual variability, which underscores the heterogeneity of the  
230 thermal regime of islands within the Lena floodplain. On the basis of field surveys and soil temperature  
231 data, we are able to distinguish two main types: islands with a perennially frozen soil (*i.e.* with a  
232 permafrost), and islands with a seasonally frozen ground only.

233

### 234 4.1. Islands with permanently frozen soil

235

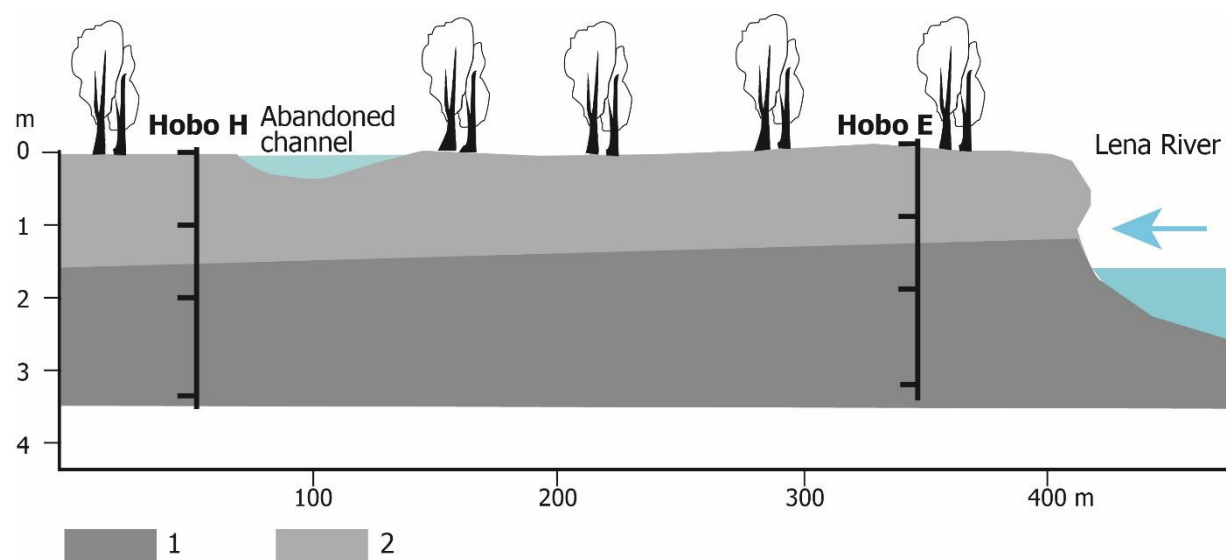
#### 236 *Eselyakh Island*

237

238 The Eselyakh Island (Figure 5) has a permanently frozen soil. According to Hobo E (Figure 6), the annual  
239 average temperature at 3.2 m depth was -2.2°C for 2009-2010 and -3°C for 2010-2011. At 1 m and 2  
240 m depths, the Hobo recorded a slightly lower mean temperature and a higher intra-annual variability  
241 (1m: -2.5°C in 2009-2010 and -4.3°C in 2010-2011; 2m: -2.4°C in 2009-2010 and -3.5°C in 2010-2011).  
242 Hobo measurements coupled with successive field campaigns have shown that the active layer is  
243 thinner on the upstream section (1.2 m depth) of the island than on the downstream section (1.5 m  
244 depth) (Figure 5). The active layer is composed of peaty sandy loam with a volumetric moisture content  
245 of 25% to 53%. Based on drilling operations, the permafrost table at Hobo E site is located at 1.5 m and  
246 contains ice-rich sandy loam materials with 19% to 50% ice content by volume.

247

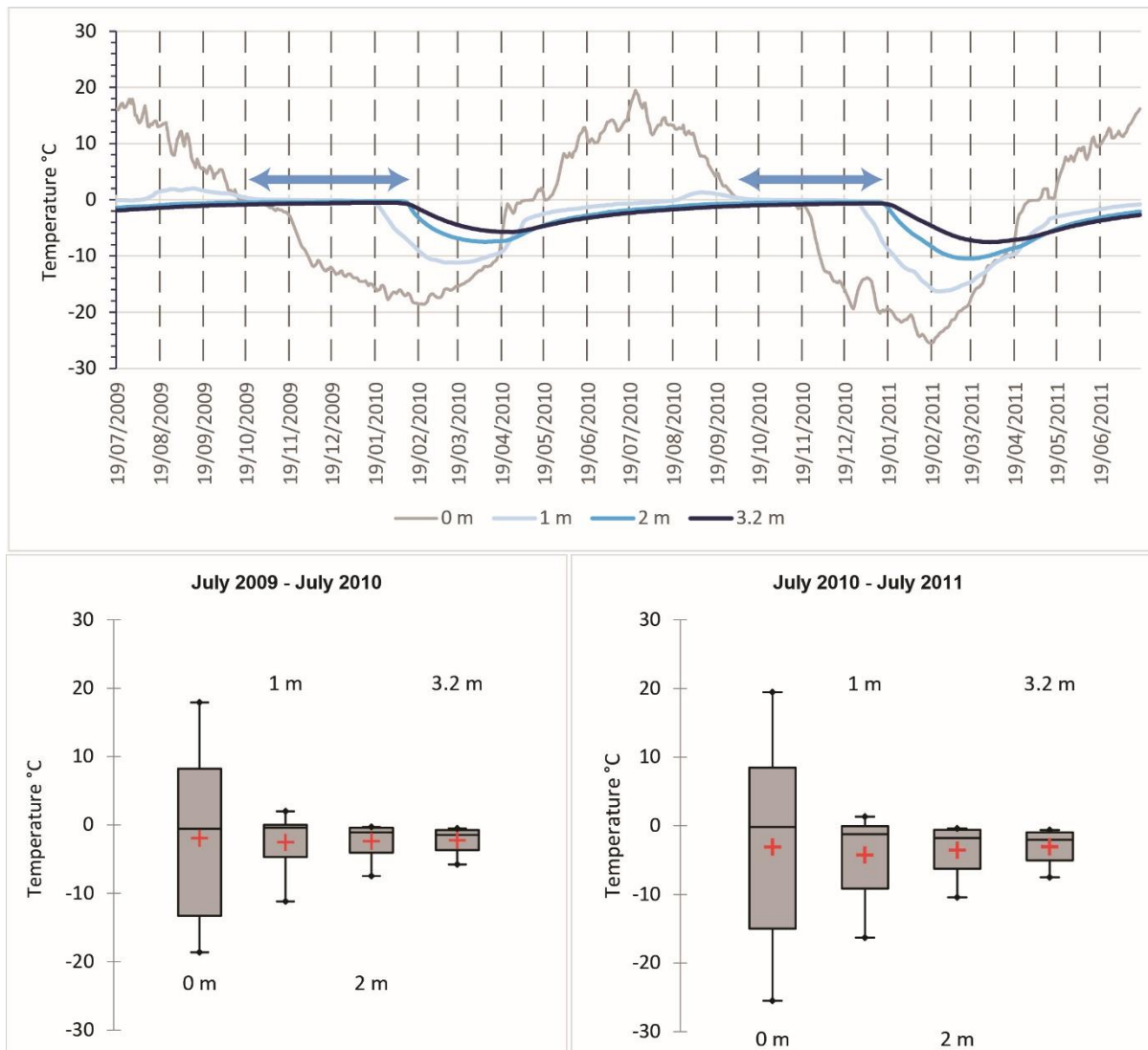
248



249  
 250 Figure 5: Schematic longitudinal section of Eselyakh Island. 1: permanent frozen soil; 2: active layer.  
 251 Blue arrow indicates flow direction (to the North). Hobo H is located near a 30 m wide abandoned  
 252 channel.

253  
 254 According to the thermal profile of HOBO E (Figure 6), underneath the active layer, there is  
 255 permanently frozen soil with temperatures ranging from  $-0.3^{\circ}\text{C}$  to  $-10.4^{\circ}\text{C}$  at a depth of 2 m during the  
 256 two consecutive years (2009 – 2010 and 2010 – 2011). At 3.2m depth, the variability of frozen soil  
 257 temperature was even less pronounced, ranging between  $-0.5^{\circ}\text{C}$  and  $-7.5^{\circ}\text{C}$ . We note a downward  
 258 propagation of the winter freezing wave and a time lag with depth for reaching minimum temperature  
 259 due to the thermal inertia of frozen ground (Figure 6). For example, the minimum annual temperature  
 260 was reached in mid-February at the soil surface, in early March at a depth of 1 m, in late March at 2 m,  
 261 and in mid-April at 3.2 m, during the first winter. The second winter was harsher and a colder weather  
 262 occurred earlier with  $-20^{\circ}\text{C}$  in December and  $-25^{\circ}\text{C}$  in February, at the soil surface. Consequently, this  
 263  $\sim 20$ -day time lag between different depths was also observed during the second winter, although  
 264 nearly three weeks earlier than the previous year (in mid-February, early March and late March,  
 265 respectively). For the October – December period, temperatures were stabilized (70 to 80 days) just  
 266 below  $0^{\circ}\text{C}$  at a depth of 1 m due to the effect of latent heat (zero curtain effect on Figure 6). At 2m and  
 267 3.2m-depth, temperature began to decrease at the end of January.

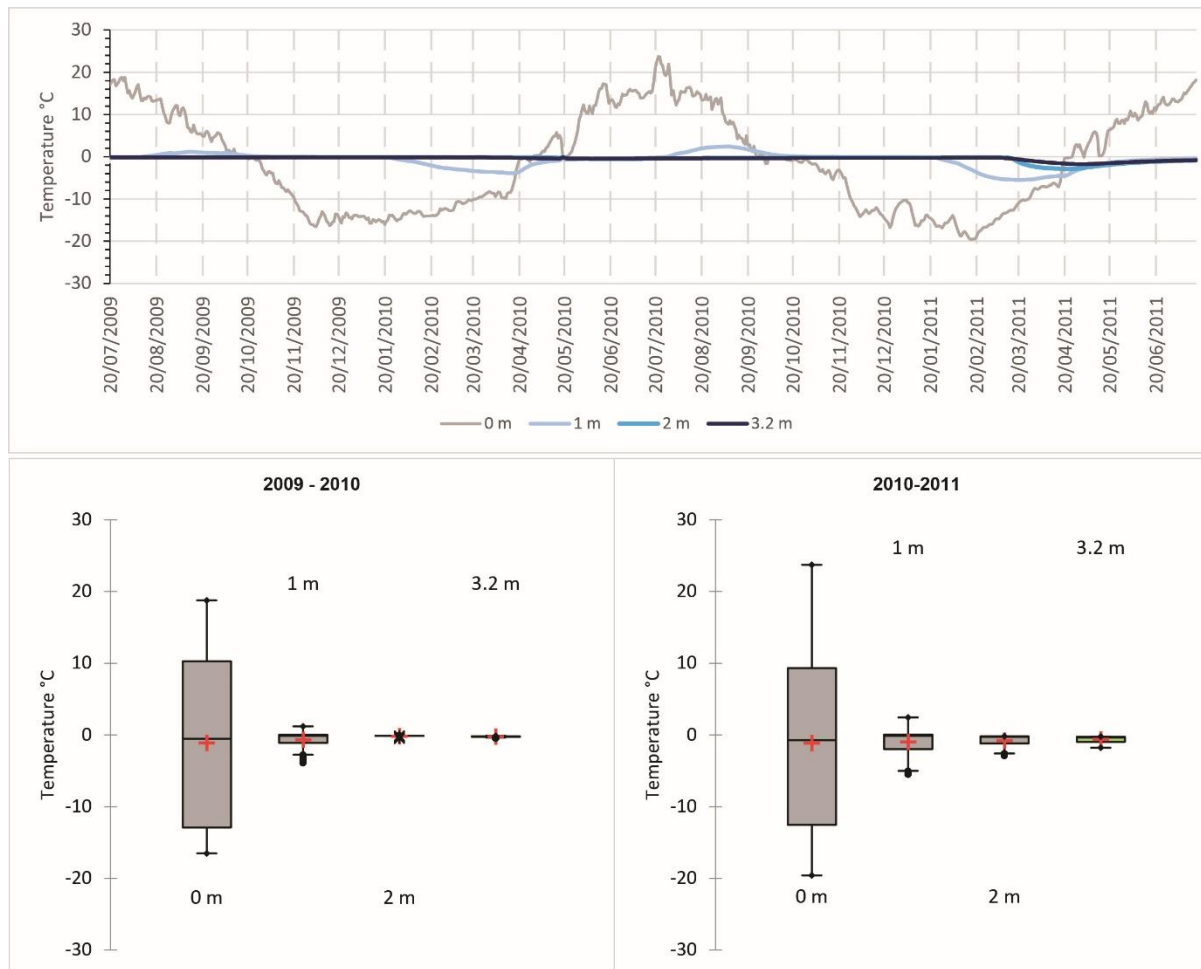
268  
 269



270  
 271 Figure 6: Ground thermal profiles on Eselyakh Island at 1 m, 2 m and 3.2 m depth for HOBO E  
 272 datalogger; 0 m: soil surface temperature (July 2009 – July 2011). Blue arrows correspond to the zero-  
 273 curtain effect during phase change of the water-ice in winter season.

274

275



276  
 277 Figure 7: Ground thermal profiles on Eselyakh Island at 1 m, 2 m and 3.2 m depth for HOBO H  
 278 datalogger; 0 m: soil surface temperature (July 2009 – July 2011).

279  
 280  
 281 Contrastingly, the thermal profile of HOBO H, located further downstream on the island (Figure 7),  
 282 shows a notably warmer frozen soil. For 2009-2010, the mean temperature was  $-0.67^{\circ}\text{C}$ ,  $-0.18^{\circ}\text{C}$  and  $-$   
 283  $0.24^{\circ}\text{C}$  at 1 m, 2 m and 3.2 m, respectively. In 2010-2011, the mean temperature was lower ( $-1^{\circ}\text{C}$ ,  $-$   
 284  $0.8^{\circ}\text{C}$ ,  $-0.6^{\circ}\text{C}$  at 1 m, 2 m and 3.2 m). Furthermore, the temperature ranged between  $\sim 0^{\circ}\text{C}$  and  $-5.5^{\circ}\text{C}$   
 285 (1 m), between  $-0.1^{\circ}\text{C}$  and  $-2.9^{\circ}\text{C}$  (2 m) and between  $-0.2^{\circ}\text{C}$  and  $-1.7^{\circ}\text{C}$  (3.2 m) during the second  
 286 (colder) winter. The temperature did not vary substantially during the first winter and decreased a bit  
 287 more during the second winter. The lowest temperature was registered in April before the breakup ( $-$   
 288  $1.8^{\circ}\text{C}$  at 3.2m). The lowest temperatures are not as cold as the one registered by Hobo E ( $-7.5^{\circ}\text{C}$  in April  
 289 2011 at 3.2 m). The sediment is identical, with the same composition and grain size characteristics as  
 290 on the previous site.

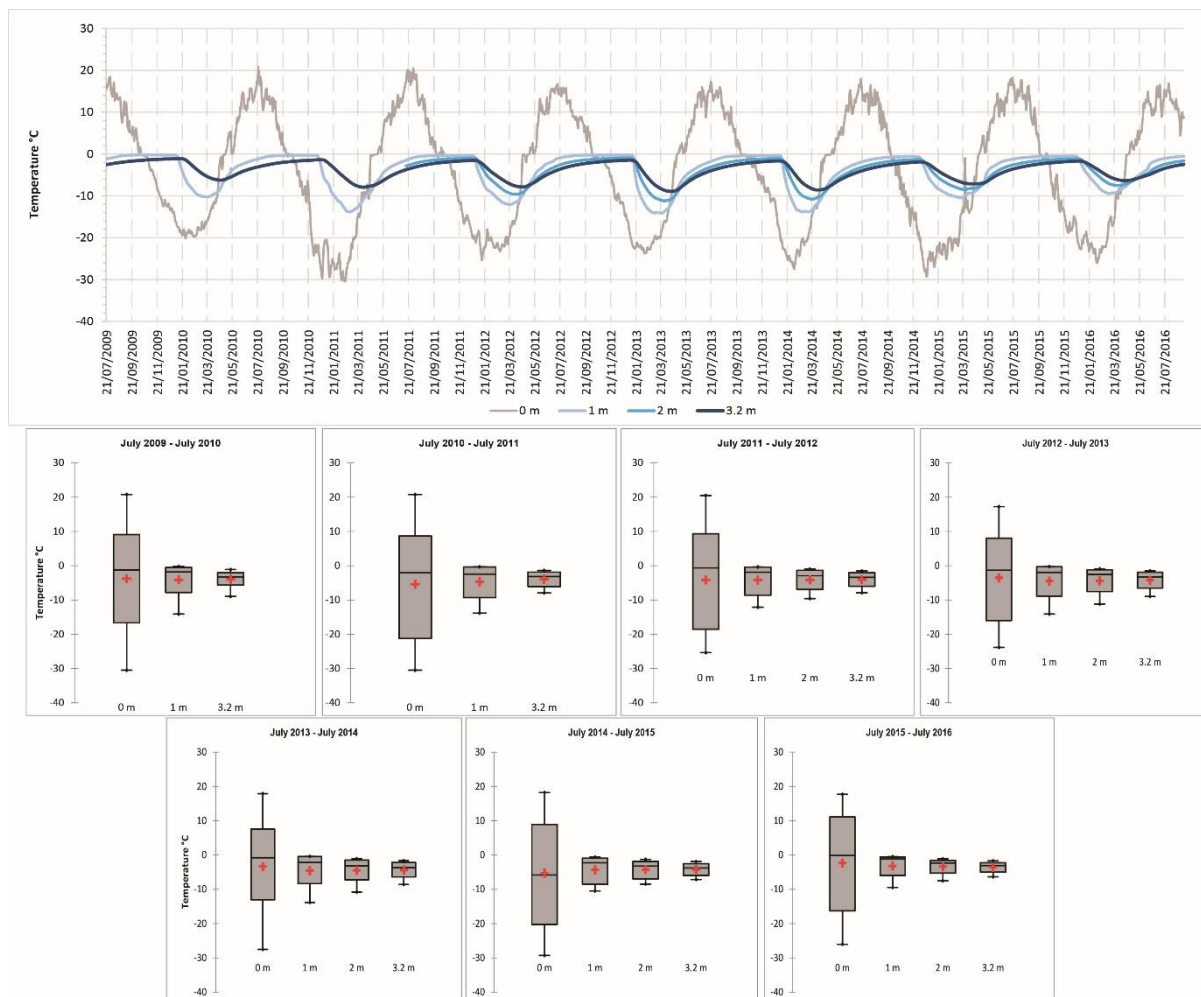
291  
 292



293 *Large lateral islands (Ynakh-Ary and Saty-Talakh)*

294 On Ynakh-Ary, Hobo I has been working from 2009 to 2016 (Figure 8). The temperature varied between  
295  $-0.1$  and  $-14^{\circ}\text{C}$  (1 m)  $-1.2^{\circ}\text{C}$  and  $-11.1^{\circ}\text{C}$  (2 m) and between  $-1.2^{\circ}\text{C}$  and  $-8.9^{\circ}\text{C}$  (3.2 m depth). When  
296 comparing the same years (2009 to 2011), Ynakkh – Ary has a colder soil than Eselyakh:  $-2.98^{\circ}\text{C}$  for  
297 2009-2010 (at 3.2 m) and  $-3.97^{\circ}\text{C}$  for 2010-2011 mean value. We also observed a two month-time-lag  
298 separating the beginning of continuous negative temperature on the soil surface (October) and the  
299 start of the cooling within the frozen soil: beginning of January at 1 m and 2 m depths, end of January  
300 or early February at 3.2m depth.

301  
302  
303



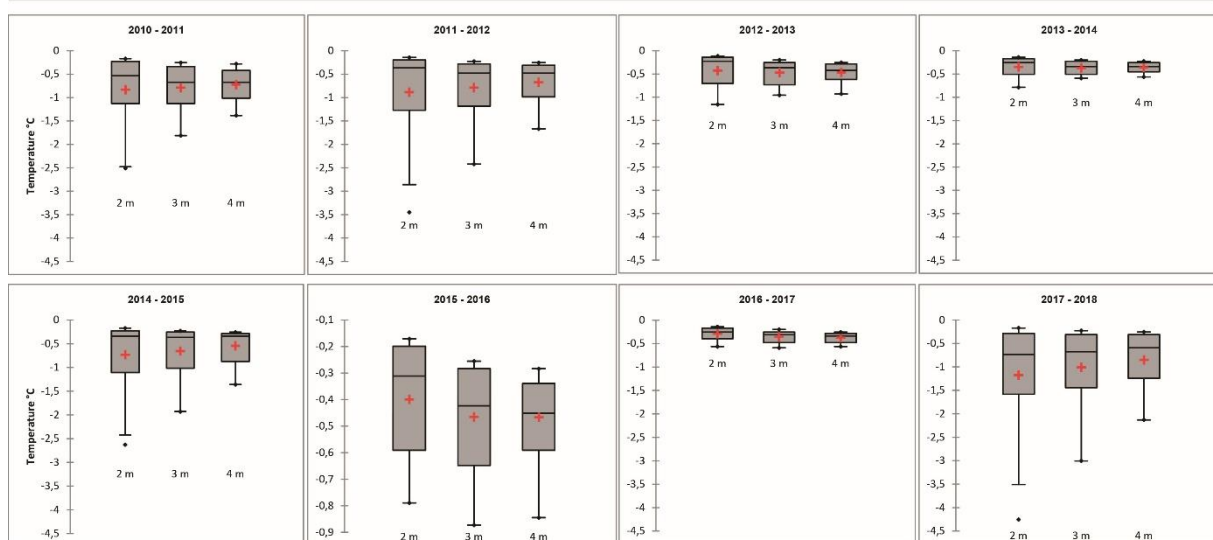
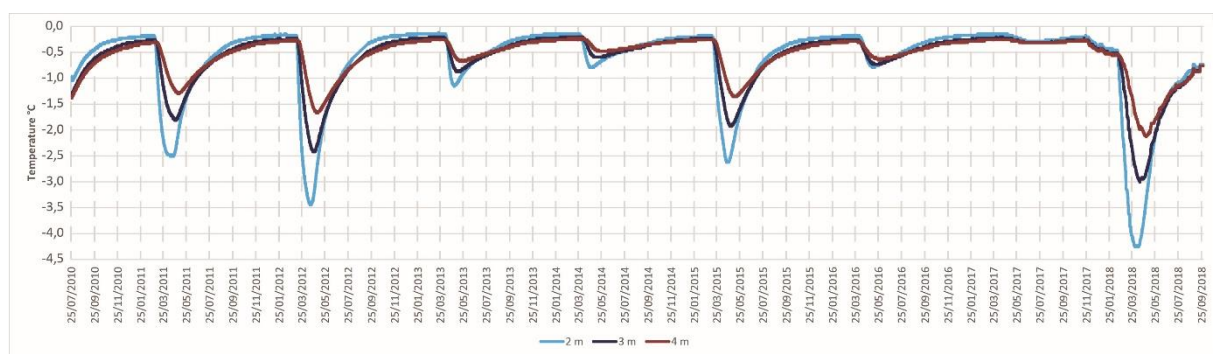
304  
305 Figure 8: Ground thermal profiles on Ynakh-Ary island, at 1 m, 2 m and 3.2 m depth for Hobo I  
306 datalogger; 0 m: soil surface temperature (July 2009 – July 2016).

307  
308 On Saty-Talakh, which is also a large lateral island, Hobo Q has been working from 2010 to 2018 (Figure  
309 9). The thermal profile differs from the data registered on Ynakh-Ary. The temperature regime is similar

310 to Hobo H on Eselyakh island, because of a relatively warm permafrost at 3.2 m depth. For 2010-2011,  
 311 the mean temperature (3.2 m) was  $-0.79^{\circ}\text{C}$  and dropped to  $-1.81^{\circ}\text{C}$  at the end of the winter. The cold  
 312 winter 2017 – 2018 induced a stronger cooling; the 3 m Hobo recorded  $-3^{\circ}\text{C}$  in mid-April.

313

314



315  
 316 Figure 9: Ground thermal profiles on Saty-Talakh island, at 2 m, 3 m and 4 m depth for Hobo Q  
 317 datalogger (July 2010 – September 2018). No data logger at the soil surface for Hobo Q.

318

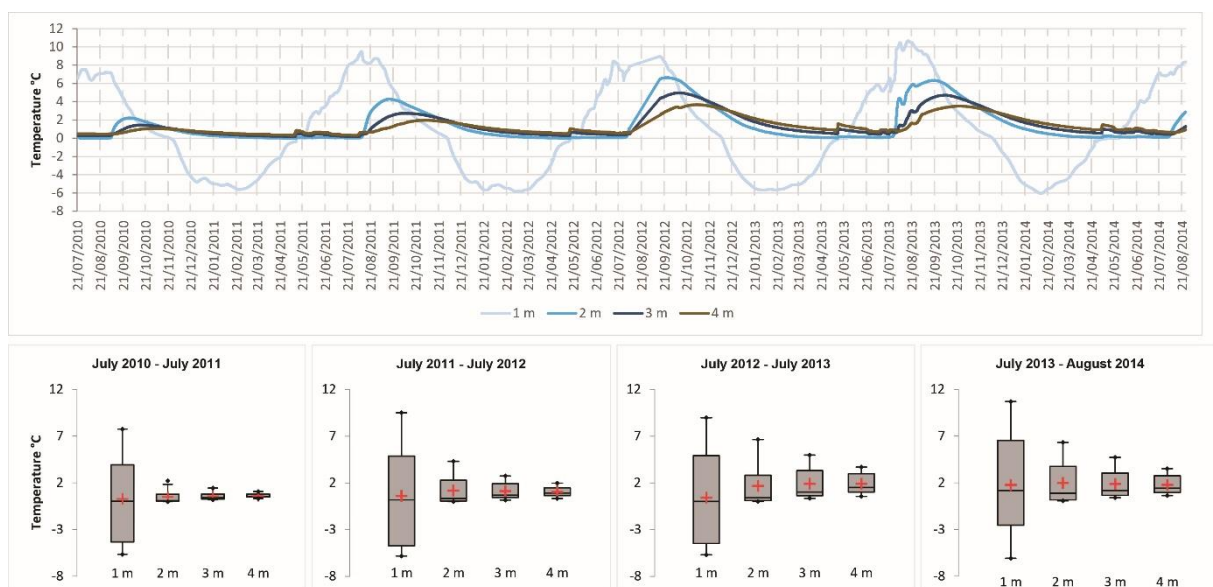
319

## 320 4.2. Islands with seasonally frozen ground

### 321 *Timochka Island*

322 Timochka Island has a seasonally frozen ground; negative temperature is observed from November to  
 323 the end of April at 1m depth. At 3.2 m depth, the average annual temperature ranges between  $+1^{\circ}\text{C}$   
 324 and  $+1.5^{\circ}\text{C}$ . Thus, temperatures remain constantly above  $0^{\circ}\text{C}$  even at a depth of 3.2 m (Figure 10). This  
 325 island is mostly composed of fine sand, and the willows are relatively younger than those on Eselyakh  
 326 Island (Gautier et al., 2021). The volumetric soil moisture content ranges from 4% at 0.1 m depth to  
 327 40% at 1 m depth. Similarly to other Hobo sites on the other islands, however, ground temperature

328 variability is notably larger near the surface (at 1 m deep) compared to several meters deep (Figure 10,  
329 lower graphs).  
330



331  
332 Figure 10: Ground thermal profiles on Timochka Island at 1 m, 2 m, 3 m and 4 m depths for HOB0-A  
333 (July 2010 – August 2014), without a permanently frozen soil. No data logger at the soil surface for  
334 Hobo A.  
335

336

## 337 5. Discussion

338 Our results demonstrate that, even in an area of thick continuous permafrost, the ground is not  
339 permanently frozen everywhere within the Lena floodplain. This study also highlights not only a strong  
340 inter-annual variability in ground temperature, but also the spatial heterogeneity of the thermal  
341 regime of frozen soils. On the one hand, some sites along the islands show a colder permafrost  
342 conditions that vary little throughout the years, and on the other hand, other sites are underlain by a  
343 notably warmer seasonally frozen ground affected by strong thermal variability. Two main factors are  
344 inferred to influence permafrost dynamics in the Lena floodplain: the age of the islands and the  
345 thermal effect of spring breakups.

346

### 347 *Age and thermal state of the islands*

348 The middle Lena River develops a multiple-channel pattern with large forested islands (Costard et al.,  
349 2000; Gautier et al., 2008). The anabranching fluvial pattern implies relative stability of the channels  
350 and islands, although some islands quickly migrate downstream. This is the case for Eselyakh and  
351 Timochka islands that are located in the central part of the active channel (Figure 1). Thus, they rapidly

352 migrate downstream, as the head is progressively eroded, whereas the tail (downstream) progresses  
353 by deposition (Figure 11). Island sides are also exposed to erosion, explaining the reduction in form  
354 size (Table 1). The two other islands (Ynakh-Ary and Saty-Talakh) are much larger lateral islands, and  
355 are more stable. As they are located at the margins of the river active channel, they are subjected to a  
356 reduced reshaping (sediment drift) with a local erosion of their bank (Figure 11).

357 Eselyakh and Timochka are relatively small islands with surface area of 0.2 km<sup>2</sup> and 0.13 km<sup>2</sup>,  
358 respectively (Table 1). They are bisected with a secondary channel between the two parts (Figure 1,  
359 Table 1). Eselyakh is older than Timochka, as its two parts were already formed in 1967 and a  
360 dendrochronological analysis of a willow puts its age at 56 years in 2010. It suggests the stabilization  
361 of a sand bar during the 1950's. The upper part of Eselyakh is progressively shrinking due to head and  
362 side erosion, whereas the lower part is growing by sedimentation. Timochka is an elongated island that  
363 is migrating very rapidly since its formation. Hence, the present-day island is young: the upper part  
364 corresponds to a deposition zone formed between 1980 and 1996.

365 Ynakh-Ary and Saty-Talakh are large islands with surface area of 5 km<sup>2</sup> and 20 km<sup>2</sup>, respectively. They  
366 had the same general shape in 1967 (Figure 11). According to local inhabitants, they are very old  
367 islands. They were formed by merging of different islands, and lakes and swamps occupy the former  
368 inter-island channels.

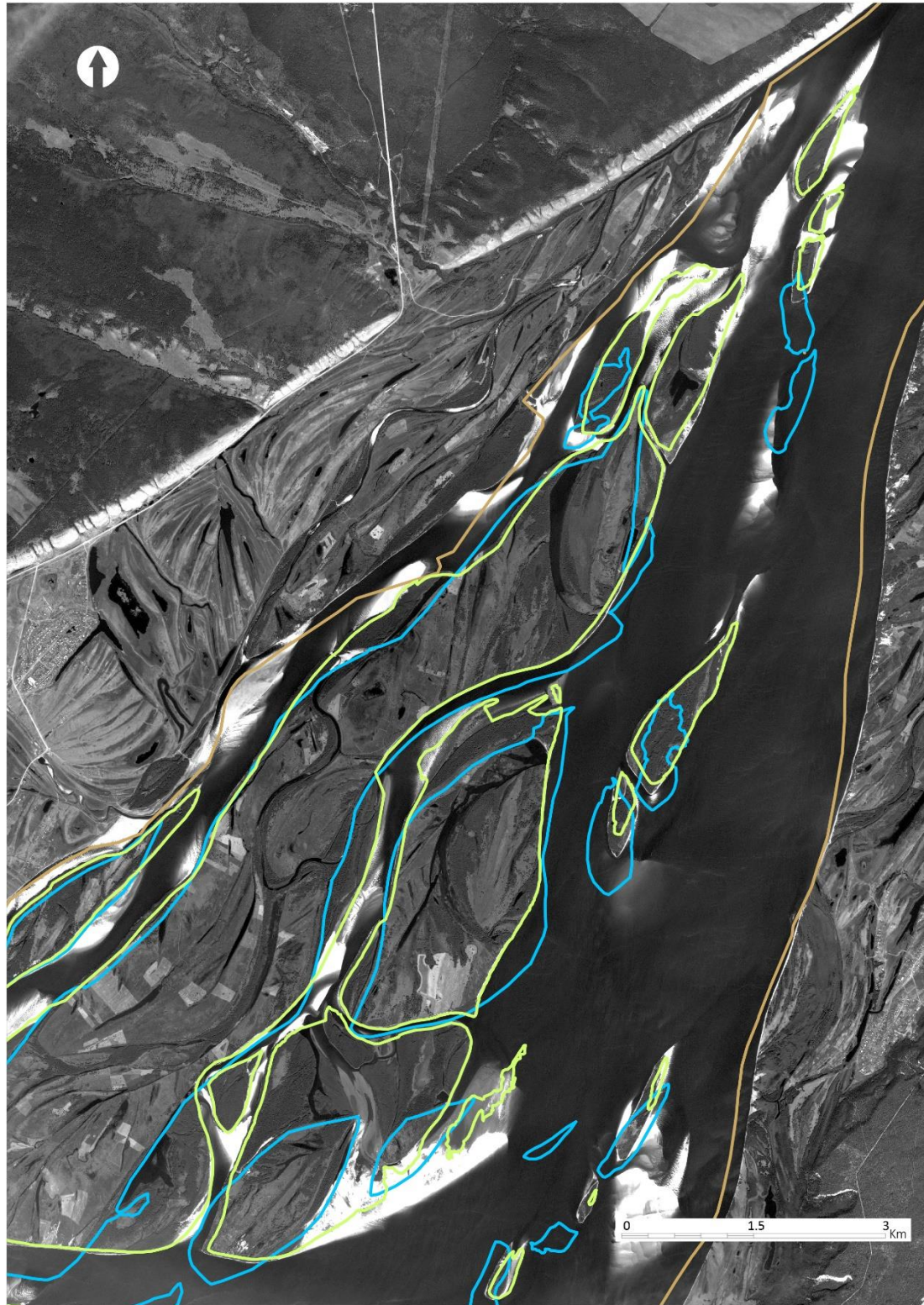
369 It appears that the oldest islands are thus at least 70 years old in our selected study area (Gautier et  
370 al., 2021). The Ynakh-Ary, Saty-Talakh and Eselyakh islands are old islands with a permanent frozen soil  
371 developed in fine-grained material (silt-clay) deposited by overbank flows overlaying a sandy base.  
372 Timochka Island is much younger, with only seasonally frozen ground and mostly sand deposits, as the  
373 island has been formed by the colonization of a former sand bar by willows. This apparent relationship  
374 between the age of deposition/formation and the thermal regime of the ground can also be extended  
375 to the much older permafrost near Yakutsk (Figure 3), where ground temperatures at 3.2 m can remain  
376 below -1°C at the end of the summer and below -4°C at the end of the winter. Contrastingly, ground  
377 temperatures barely or never attain such low values at Eselyakh (Figures. 6 and 7), Ynakh-Ary (Figure  
378 8) or Saty-Talakh (Figure 9), which are nevertheless underlain by frozen ground. Permafrost obviously  
379 had much less time to develop at these sites and is in equilibrium with current climate conditions,  
380 which is not the case 'onshore' near Yakutsk.

381 However, the age of the island is not the only parameter explaining the observed differences. Local  
382 parameters, and more precisely, abandoned channels, also seem to explain the observed thermal  
383 heterogeneity. Hobo H is located not far from a 30 m-large abandoned channel (Figure 5), which  
384 obviously induces a thermal effect by heating the upper part of the frozen soil. Widespread along the  
385 floodplain, such abandoned channels are watered more frequently and they are located on lower

386 topographic levels. These depressions are humid and occupied by swampy vegetation. Eselyakh (Hobo  
387 E) and Ynakh-Ary dataloggers are installed on higher topographic levels.

388





389  
390 Figure 11: Island migration of the study reach upstream of Yakutsk city from GIS study. Blue line: island  
391 shape in 1967 (Corona photographs); Brown line: channel bank in 1967; Green line: island shape 2017



392 (Pleiade images © CNES, 2017, Distribution Airbus DS, all rights reserved). Background image: Spot  
 393 2008 (© CNES, France)

394

395 *Thermal effect of spring breakup: the example of 2010*

396 During spring floods, the islands along the Lena River channel are submerged and this induces an  
 397 additional thermal imprint. Our dataloggers were able to record this specific stage on Eselyakh and  
 398 Ynakh-Ary islands (Figure 12). It can be seen that the temperature variations on the ground are  
 399 suddenly interrupted on May 19, 2010 with a temperature dropping and remaining at 0°C until May  
 400 25 (Figure 12; Table 2). This is due to the inundation of the islands when the flooding begins (for a  
 401 discharge exceeding about 30,000 m<sup>3</sup>.s<sup>-1</sup>). The submersion duration greatly varied during the study  
 402 period (Table 3).

403 Furthermore, the sensor installed at the soil surface (0 m on Figure 12) registered the water stream  
 404 temperature. At the beginning of the flooding, temperatures close to 0°C confirm the existence of a  
 405 mixture of water and ice during the breakup. Then, after a few days, the water temperature slightly  
 406 increases (1°C to 3°C) as the islands are inundated by water only.

407

408 Table 2. Flood duration, number of flood peaks and temperature range of the study sites along the  
 409 Lena River

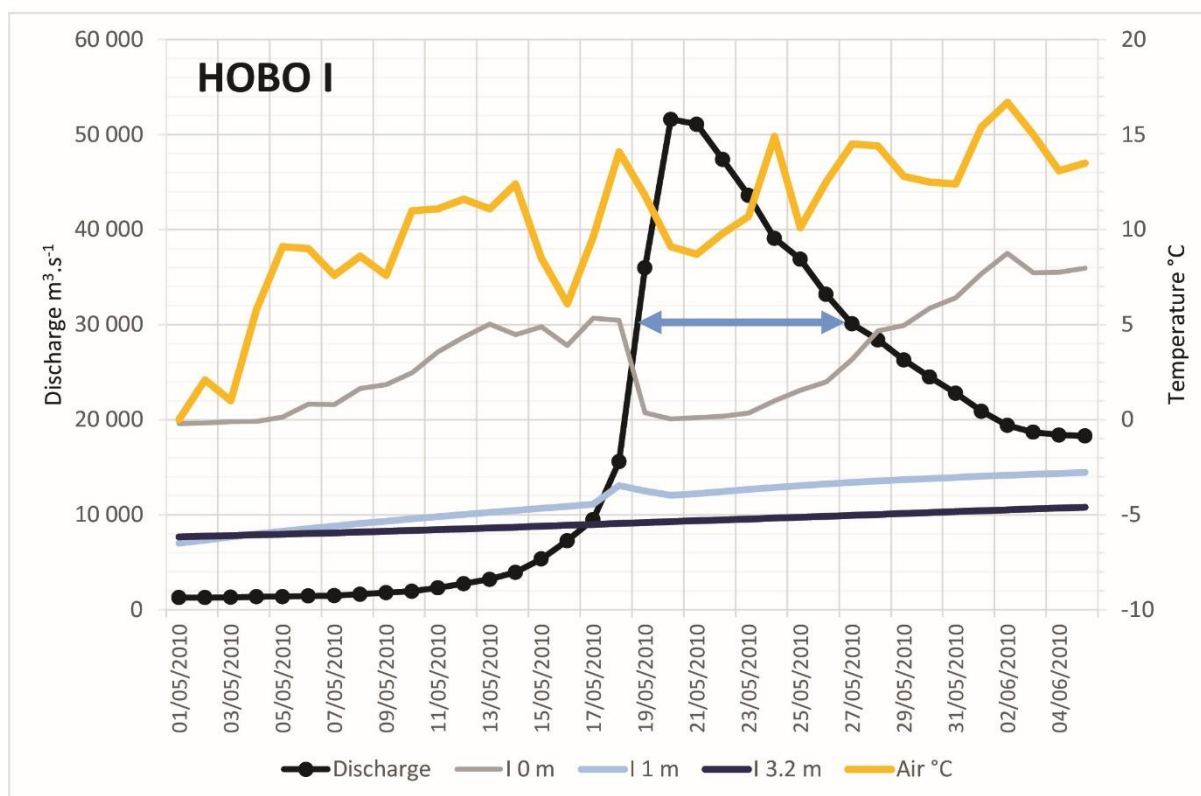
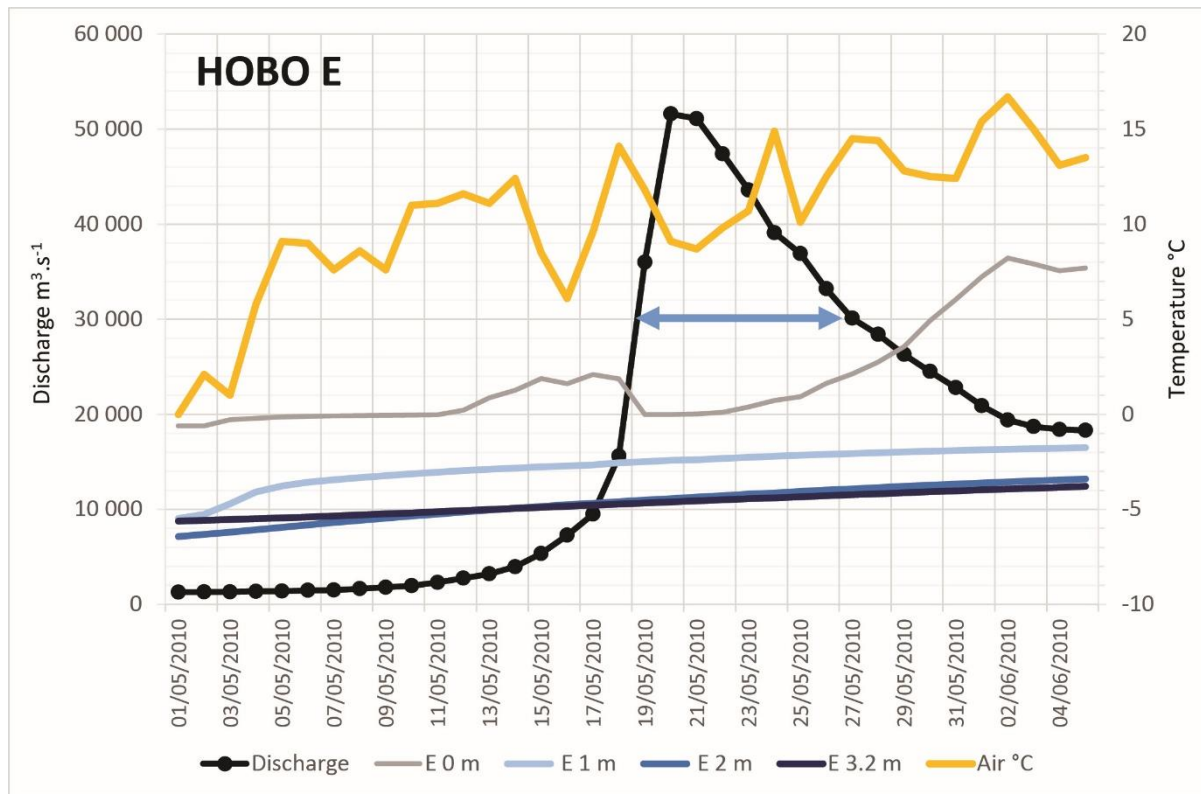
410

	Flooding duration (Days)	Flood peaks	Stream water temperature range (°C)
2009	26	June 3 <sup>rd</sup> – June 28 <sup>th</sup>	ND
2010	9	May 19 <sup>th</sup> – May 27 <sup>th</sup>	0°C – 0.9°C
2011	6	May 13 <sup>th</sup> – May 18 <sup>th</sup>	0.2°C – 1.4°C
2012	36	May 17 <sup>th</sup> – May 26 <sup>th</sup> June 5 <sup>th</sup> – June 19 <sup>th</sup> July 5 <sup>th</sup> – July 9 <sup>th</sup> July 28 <sup>th</sup> – August 4 <sup>th</sup>	0°C – 3°C 9.5°C – 12°C 15°C – 15.5°C 15°C – 16.5°C
2013	14	May 14 <sup>th</sup> – May 21 <sup>st</sup> July 23 <sup>rd</sup> – July 29 <sup>th</sup>	5°C – 5.5°C 18°C – 19°C
2014	0		
2015	7	May 13 <sup>th</sup> – May 19 <sup>th</sup>	0.3°C – 3°C
2016	10	June 10 <sup>th</sup> – June 16 <sup>th</sup>	11.6°C – 13.3°C

		July 31 <sup>st</sup> – August 3 <sup>rd</sup>	14.6° – 15°C
2017	5	July 20 <sup>th</sup> – July 24 <sup>th</sup>	19°C – 19.5°C
2018	17	May 5 <sup>th</sup> – May 10 <sup>th</sup> July 19 <sup>th</sup> – July 25 <sup>th</sup>	ND

411  
412 However, the observed effect of island submersion at the time of breakup appears to have a relatively  
413 moderate impact on thermal profile at depth (i.e. more than 1 m deep). This can likely be explained by  
414 1) the duration of submersion, which in that case is too short to have a long-term thermal impact in  
415 the ground, and 2) the water temperature, still near 0°C, again precluding major thermal disturbance  
416 within the ground, at least below the surface. Figure 12 clearly shows that the ground temperature  
417 regime for the two islands (Eselyakh and Ynakh-Ary) did not change, even during the 10-day  
418 submersion of the island during the ice breakup in May.

419  
420  
421  
422



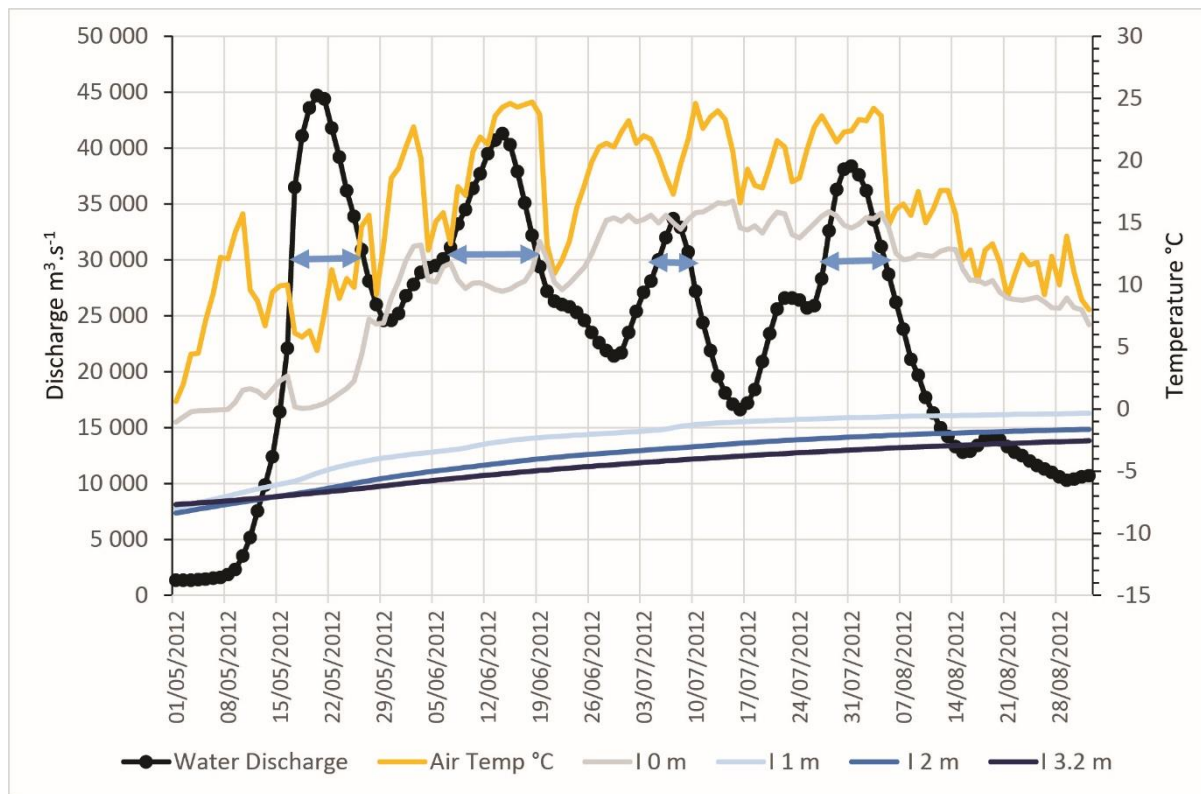
423  
 424 Figure 12: Mean daily discharge and temperature on islands with a permanent frozen soil (2010, May  
 425 1 – June 5). Eselyakh Island (HOBO E), Ynakh-Ary Island (Hobo I). Water Discharge at Tabaga gauging  
 426 station (Roshydromet data); 0 m: soil surface temperature; ground temperature at different depths (1

427 m, 2 m and 3.2 m); air temperature at Yakustk (NOAA, NASA data). The blue arrow corresponds to the  
428 submersion duration of the islands in relation with a discharge  $> 30,000 \text{ m}^3 \cdot \text{s}^{-1}$ .

429  
430 Interestingly, multiple water level increases during the warm seasons have occurred in the Lena River.  
431 During some years, the islands can be inundated twice or more often. For example, in 2012, the Lena  
432 River underwent four flood peaks (Figure 13) with 36 days of total flood duration (Table 2). The  
433 repeated inundations and warm stream water did not significantly affect, however, the ground  
434 temperature regime of the islands.

435 Regarding the surface temperature recorded in 2010 and in 2012 for Eselyakh Island (HOBO E) and  
436 Ynakh-Ary Island (Hobo I), we can observe a systematic decrease of the surface temperature (0 m)  
437 during each of these breakups and flood seasons (Figures 12 and 13). The water stream temperature  
438 is systematically lower than the air temperature due to the water/ice mixture of the breakup that  
439 decreases the surface temperature of the islands during the submersion phase. We also observed that  
440 the initial phase of the breakup in May is accompanied by a net decrease in air temperature (yellow  
441 curve on figure 12 and figure 13). Finally, regardless of the water stream temperature or the thermal  
442 state and water/ice content of the subsoil, the thermal regime of the subsoil at 1 m depth (Figure 13)  
443 does not appear to be affected.

444  
445



446

447 Figure 13: Mean daily discharge, air temperature and thermal regime of subsoil of Ynakh-Ary (HOBO I)  
448 between May and August 2012. Water Discharge at Tabaga gauging station (Roshydromet data); 0 m:  
449 soil surface temperature; ground temperature at different depths (1 m, 2 m and 3.2 m); air  
450 temperature at Yakutsk (NOAA, NASA data). Blue horizontal line corresponds to a water discharge >  
451 30,000 m<sup>3</sup>.s<sup>-1</sup> in relation with the submersion of the island.

452

## 453 **6. Conclusion**

454 For a first time, we were able to instrument a large Arctic fluvial system in order to acquire new data  
455 on frozen ground development within a large floodplain. Our measurement campaigns revealed that  
456 the floodplain of the Lena River, upstream of Yakutsk, does not everywhere contain permanently  
457 frozen soil, and that some highly mobile and young islands have (only) a seasonally frozen ground.  
458 Even in old islands, where frozen ground is present, a marked variability is noticeable. We also conclude  
459 that the ice breakups and floods seem to have a negligible impact on the ground thermal regime. Our  
460 study confirms that relatively young (less than 50 years old) islands, composed of fine sand material,  
461 appear less prone to permafrost formation compared to older islands with ice-rich silty material. Thus,  
462 the Lena floodplain is notably heterogeneous, with a combination of permanently and seasonally  
463 frozen islands. The observed disparity between these islands is significant and unexpected, because it  
464 confirms that the Lena River floodplain is far from being thermally and geomorphologically  
465 homogenous. It rather consists of a juxtaposition of seasonally frozen islands and permanently frozen  
466 islands in the regional context of a floodplain affected by thick and continuous permafrost. The  
467 heterogeneity could also induce differential responses of the frozen and unfrozen parts of the  
468 floodplain to global warming.

469

## 470 **Acknowledgements**

471 This program was funded by ANR programs 'CLIMAFLU' (CLIMAtic change and FLUvial dynamic of the  
472 Lena River, Siberia) and 'MOPGA' (Make Our Planet Great Again; through 'Projet d'Investissements  
473 d'Avenir'), coordinated at GEOPS (Géosciences Paris-Saclay), Université Paris-Saclay. It also includes  
474 collaborations with LGP (Laboratoire de Géographie Physique, Meudon) in France and the Melnikov  
475 Permafrost Institute (Yakutsk) in Russia. All data from our field studies are presented in the  
476 supplementary material S1 to S4. We gratefully thank Tomáš Uxa and an anonymous reviewer for their  
477 constructive comments.

478

479

## 480 **References :**

481 Antonov, S., 1960. Delta reki Leny. Trudy Okeanographicheskoy Komissii. Ak. Nauk. SSSR, 6: 25-34.

482  
483 Are, F.E. (1983), Thermal abrasion on coasts, Proceedings, Fourth International Conference on  
484 Permafrost, Fairbanks, Alaska, National Academy Press, Washington DC, 24-28.  
485  
486 Beltaos, S. and B. C. Burrell (2002), Suspended sediments concentrations during the spring breakup of  
487 river ice.. In Ice in Surface Waters, Proceedings of the 14th IAHR Ice Symposium, 27-31 July 1998,  
488 Postdam, N.Y. Edited by H.T. Shen. A.A. Balkema, Rotterdam, 2, 793-800.  
489  
490 Billfalk, L. (1982), Breakup of solid ice covers due to rapid water level variations. CRREL Report 82-3,  
491 US Army CRREL, Hanover, N.H.  
492  
493 Biskaborn et al. 2019. Permafrost is warming at a global scale. Nature Communications, 10, 264. doi:  
494 s41467-018-08240-4.  
495  
496 Costard F., E. Gautier, D. Brunstein, J. Hammadi, A. Fedorov, D. Yang, L. Dupeyrat (2007). Impact of the  
497 global warming on the fluvial thermal erosion over the Lena river in Central Siberia. Geophys. Res.  
498 Lett., 34, (14), doi:10.1029/2007GL030212  
499  
500 Costard F. and Gautier E. (2007). The Lena River: main hydromorphodynamic features in a deep  
501 permafrost zone. In Large rivers: Geomorphology and Management, Gupta A (ed.). John Wiley & Sons;  
502 225-232.  
503  
504 Costard F., E. Gautier, A. Fedorov, P. Konstantinov and L. Dupeyrat. (2014). An assessment of the  
505 erosional potential of fluvial thermal process during ice breakups of the Lena River (Siberia).  
506 Permafrost and Periglacial Processes, Vol. 25, 162-171, doi:10.1002/ppp.1812  
507  
508 Dupeyrat, L., Hurault, B., Costard, F., Marmo, C., Gautier, E., (2018). Satellite image analysis and frozen  
509 cylinder experiments on thermal erosion of periglacial fluvial islands. Permafr. Periglac. Process.  
510 doi:10.1002/ppp.1973  
511  
512 Fedorov, A. and P. Konstantinov (2003), Observations of surface dynamics with thermokarst initiation,  
513 Yukechi site, Central Yakutia. Proceedings of International Permafrost Conference, Zurich, In  
514 Permafrost, Philips M., Springman S. Arenson L.U. (eds), 239-243.  
515



516 Fedorov, A.N., Ivanova, R.N., Park, H., Hiyama, T., Iijima, Y., 2014. Recent air temperature changes in  
517 the permafrost landscapes of northeastern Eurasia. *Polar Sci.* 8, 114–128.  
518 doi:10.1016/j.polar.2014.02.001  
519

520 Gautier, E. and F. Costard (2000), Les systèmes fluviaux à chenaux anastomosés en milieu périglaciaire:  
521 la Léna et ses principaux affluents en Sibérie Centrale. *Géographie Physique et Quaternaire*, 54/3, 327-  
522 342.  
523

524 Gautier, E., D. Brunstein, F. Costard and R. Lodina (2003), Fluvial dynamics in a deep permafrost zone:  
525 the case of the middle Lena River (Central Yakutia). *Proceedings of International Permafrost*  
526 *Conference, Zurich, Philips M., Springman S. Arenson L.U. (eds), 271-275.*  
527

528 Gautier E., A. Fedorov, F. Costard and D. Brunstein (2011). Impact of climate change on the dynamics  
529 of a large Russian Arctic river, the Lena in Central Siberia. In *Le changement climatique. Fourth Evian*  
530 *European Dialogues. EURCASIA Ed. pp. 65-73.*  
531

532 Gautier, Emmanuèle, Dépret, T., Costard, F., Virmoux, C., Fedorov, A., Grancher, D., Konstantinov, P.,  
533 Brunstein, D. (2018). Going with the flow: Hydrologic response of middle Lena River (Siberia) to the  
534 climate variability and change. *J. Hydrol.* 557, 475–488. doi:10.1016/j.jhydrol.2017.12.034  
535

536 Gautier E., Depret Th., Caverio J., Costard F., Virmoux C., Fedorov A., Konstantinov P., Jammet M., and  
537 D. Brunstein (2021). Fifty-year dynamics of the Lena river islands (Russia): spatio-temporal pattern of  
538 large periglacial anabranching river and influence of climate change. *Science of the Total Environment*.  
539 783, 147020. [doi.org/10.1016/j.scitotenv.2021.147020](https://doi.org/10.1016/j.scitotenv.2021.147020)  
540

541 Iijima, Y., Fedorov, A. N., Park, H., Suzuki, K., Yabuki, H., Maximov, T. C., and Ohata, T., 2010. Abrupt  
542 increases in soil temperatures following increased precipitation in a permafrost region, central Lena  
543 river basin, Russia. *Permafrost and Periglacial Processes*, 21(1):30–41.  
544

545 Iijima, Y., Nakamura, T., Park, H., Tachibana, Y., Fedorov, A.N., 2016. Enhancement of Arctic storm  
546 activity in relation to permafrost degradation in eastern Siberia. *Int. J. Climatol.* 2007.  
547 doi:10.1002/joc.4629  
548

549 Jahn, A. (1975), *Problems of the periglacial zone*, Washington D.C., Warszawa, 223 p.  
550

551 Konstantinov, P.Y., A.N. Fedorov, T. Nachimura, G. Iwahana, H. Yabuki, Y. Iijima, F. Costard (2011). Use  
552 of automated recorders (data loggers) in permafrost temperature monitoring. *Kriosphera Zemli*, 1, 23-  
553 32, in Russian.

554

555 Liu B., D. Yang, B. Ye, and S. Berezovskaya (2005), Long-term open-water season stream temperature  
556 variations and changes over Lena River Basin in Siberia. *Global and Planetary Change*, 48, 1-3, 96-111.

557

558 Peterson, B.J., R. M. Holmes, J. W. McClelland, C. J. Vörösmarty, R. B. Lammers, A.I. Shiklomanov, I. A.  
559 Shiklomanov, and S. Rahmstorf, (2002), Increasing River discharge to the Arctic Ocean. *Nature*, 298,  
560 2171-2173. doi:10.1126/science.1077445

561

562 Shen, H.T. (2003), Research on river ice processes: progress and missing links. *J. Cold Regions*  
563 *Engineering*, 135-142.

564

565 Schirrmeister, L., Froese, D., Tumskey, V., Grosse, G., and Wetterich, S. (2013). "Yedoma: late  
566 Pleistocene ice-rich syngenetic permafrost of Beringia," in *The Encyclopedia of Quaternary Science*, ed.  
567 S. A. Elias (Amsterdam: Elsevier), 542–552. doi: 10.1016/b978-0-444-53643-3.00106-0

568

569 Shiklomanov, A.I., Lammers, R.B., (2009). Record Russian river discharge in 2007 and the limits of  
570 analysis. *Environ. Res. Lett.* 112, 1–14. doi:10.1029/2006JG000352

571

572 Soloviev, P.A. (1973). Thermokarst phenomena and landforms due to frost heaving in Central Yakutia.  
573 *Biul. Peryglac.* 23: 135-155.

574

575 Tananaev, N.I., (2016). Hydrological and sedimentary controls over fluvial thermal erosion, the Lena  
576 River, central Yakutia. *Geomorphology* 253, 524–533. doi:10.1016/j.geomorph.2015.11.009

577

578 Tei, S., Morozumi, T., Nagai, S., Takano, S., Sugimoto, A., Shingubara, R., Fan, R., Fedorov, A.,  
579 Gavrilyeva, T., Tananaev, N., Maximov, T. (2020). An extreme flood caused by a heavy snowfall over  
580 the Indigirka River basin in Northeastern Siberia. *Hydrol. Process.* 34, 522–537. doi:10.1002/hyp.13601

581

582 Walker, H.J. (1983). Erosion in a permafrost dominated delta, *Proceedings Fourth International*  
583 *Conference on Permafrost, Alaska*. National Academy Press, Washington DC, 1344-1349.

584

585 Walker, H.J. and P. F. Hudson (2003), Hydrologic and Geomorphic Processes in the Colville Delta,  
586 Alaska. *Geomorphology*, 56, 291-303. doi:10.1016/S0169-555X(03)00157-0  
587  
588 Yang D., D. Kane, L. Hinzman, X. Zhang, T. Zhang, and H. Ye (2002), Siberian Lena River hydrologic  
589 regime and recent change. *J. of Geophys. Res.* , 107 (D23), 4694-4703. doi:10.1029/2002JD002542  
590  
591 Zhang, X., He, J., Zhang, J., Polyakov, I., Gerdes, R., Inoue, J., Wu, P. (2012). Enhanced poleward  
592 moisture transport and amplified northern high-latitude wetting trend. *Nat. Clim. Chang.* 3, 47–51.  
593 doi:10.1038/nclimate1631  
594